What does Color Glass Look Like?

What does it predict for A+A?

Cartoons vs Mathematica 4.0

M. Gyulassy: ITP/UCSB Discussion 5/24/02

Motivation: EKRT vs KLN vs KV vs McV vs Poly-Unsaturated Models (HIJING ...) Vs STAR, PHENIX, PHOBOS, BRAHMS

"Surrealism - To make the abnormal look normal and the normal look abnormal." - Salvador Dali

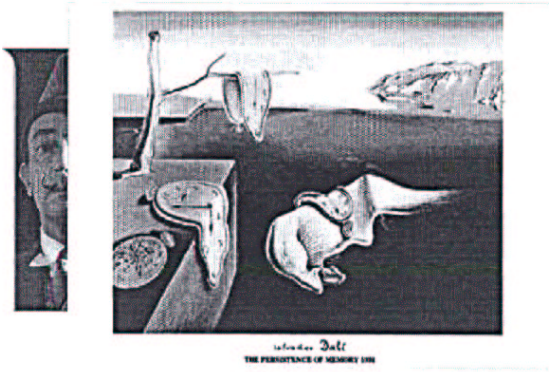

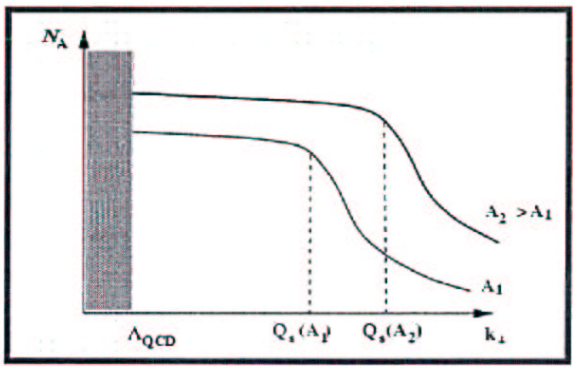

3) MANIFESTATIONS OF HIGH DENSITY QCD IN THE FIRST RHIC DATA.

By Dmitri Kharzeev (Brookhaven), Eugene Levin (Tel Aviv U.). BNL-NT-01-18, Aug 2001.
Published in **Phys.Lett.B523:79-87,2001**

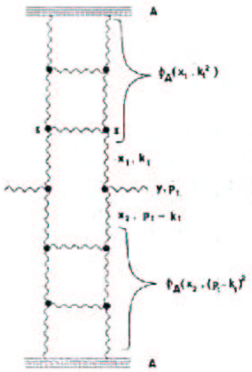

The differential cross section of gluon production in a AA collision can now be written down as [1, 23]

$$E\frac{d\sigma}{d^3p} = \frac{4\pi N_c}{N_c^2-1}\,\frac{1}{p_t^2}\int dk_t^2\;\alpha_s\;\varphi_A(x_1,k_t^2)\;\varphi_A(x_2,(p-k)_t^2), \tag{20}$$

where $x_{1,2} = (p_t/\sqrt{s})\exp(\pm\eta)$, with η the (pseudo)rapidity of the produced gluon; the running coupling α_s has to be evaluated at the scale $Q^2 = max\{k_t^2,(p-k)_t^2\}$. The rapidity density is then evaluated from (20) according to

$$\frac{dN}{dy} = \frac{1}{\sigma_{AA}}\int d^2p_t\left(E\frac{d\sigma}{d^3p}\right), \tag{21}$$

where σ_{AA} is the inelastic cross section of nucleus–nucleus interaction.

$$xG_A(x,p_t^2) = \int^{p_t^2} dk_t^2\;\varphi_A(x,k_t^2); \tag{17}$$

when $p_t^2 > Q_s^2$, the unintegrated distribution corresponding to the bremsstrahlung radiatio spectrum is

$$\varphi_A(x,k_t^2) \sim \frac{\alpha_s}{\pi}\,\frac{1}{k_t^2}. \tag{18}$$

In the saturation region, the gluon structure function is given by (8); the corresponding uni tegrated gluon distribution has only logarithmic dependence on the transverse momentum:

$$\varphi_A(x,k_t^2) \sim \frac{S_A}{\alpha_s};\; k_t^2 \le Q_s^2, \tag{19}$$

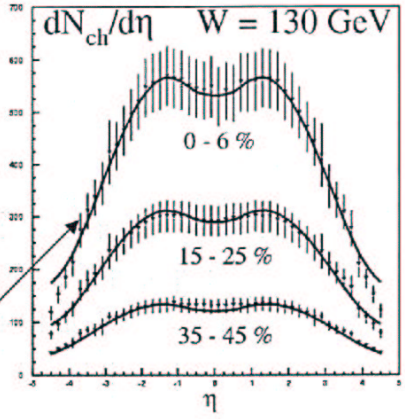

Assumed cartoon: $\varphi_A = \dfrac{\pi R^2}{\alpha_s(Q_s^2)}\,\theta(Q_s^2 - k^2)$

Classical Yang-Mills Model (McLerran-Venugopalan)

$$xG(x,Q^2) = \int^{Q^2} d^2k_\perp\,k^+\frac{dN}{dk^+d^2k_\perp}\bigg|_{k^+=xP^+}$$

$$A_c^i(x^+,\vec{x}) = \int_{k^+>0}\frac{d^3k}{(2\pi)^3 2k^+}\left(e^{i\vec{k}\cdot\vec{x}}a_c^i(x^+,\vec{k}) + e^{-i\vec{k}\cdot\vec{x}}a_c^{i\dagger}(x^+,\vec{k})\right) \tag{2.13}$$

$(\vec{x}\cdot\vec{k} = x^-k^+ - \mathbf{x}_\perp\cdot\mathbf{k}_\perp)$ with the creation and annihilation operators satisfying the following commutation relation at equal LC time x^+ :

$$[a_b^i(x^+,\vec{k}),a_c^{j\dagger}(x^+,\vec{q})] = \delta^{ij}\delta_{bc}\,2k^+(2\pi)^3\delta^{(3)}(k-q). \tag{2.14}$$

In terms of these Fock space operators, the gluon density is computed as:

$$\frac{dN}{d^3k} = \langle a_c^{i\dagger}(x^+,\vec{k})\,a_c^i(x^+,\vec{k})\rangle = \frac{2k^+}{(2\pi)^3}\langle A_c^i(x^+,\vec{k})A_c^i(x^+,-\vec{k})\rangle, \tag{2.15}$$

LC-gauge, $F_a^{i+}(k) = ik^+A_a^i(k)$, one obtains (with $k^+ = xP^+$):

$$xG(x,Q^2) = \frac{1}{\pi}\int\frac{d^2k_\perp}{(2\pi)^2}\,\Theta(Q^2-k_\perp^2)\left\langle F_a^{i+}(\vec{k})F_a^{i+}(-\vec{k})\right\rangle.$$

We shall need later also the gluon distribution function in the transverse phase-space (in short, the "gluon density"), i.e., the number of gluons per unit rapidity per unit transverse momentum per unit transverse area:

$$\mathcal{N}_\tau(k_\perp,b_\perp) \equiv \frac{d^5N}{d\tau d^2k_\perp d^2b_\perp} = \frac{d^2\,xG(x,k_\perp^2)}{d^2k_\perp d^2b_\perp}, \tag{2.21}$$

where $\tau = \ln(1/x) = \ln(P^+/k^+)$ and $b_\perp$ is the impact parameter in the trans-

E. Iancu, et al hep-th/0202270

$$\mathcal{N}_\tau(k_\perp) = \frac{1}{\pi R^2}\frac{d^3N}{d\tau d^2k_\perp} = \frac{1}{4\pi^4 R^2}\langle F_a^{i+}(\vec{k})F_a^{i+}(-\vec{k})\rangle$$

$$\boxed{\langle \mathcal{F}_a^{i+}(\vec{k})\mathcal{F}_a^{i+}(-\vec{k})\rangle_A \simeq \frac{1}{k_\perp^2}\langle \rho_a(\vec{k})\rho_a(-\vec{k})\rangle_A = \pi R_A^2(N_c^2-1)\frac{\mu_A}{k_\perp^2}}$$

$$\boxed{\begin{aligned} \mathcal{N}_A(k_\perp) &\simeq \frac{N_c^2-1}{4\pi^3}\frac{\mu_A}{k_\perp^2}, \qquad (2.55)\\ xG(x,Q^2) &\simeq \frac{(N_c^2-1)R_A^2}{4\pi}\mu_A\int_{\Lambda_{QCD}^2}^{Q^2}\frac{dk_\perp^2}{k_\perp^2} = \frac{\alpha_s A N_c C_f}{\pi}\ln\frac{Q^2}{\Lambda_{QCD}^2}, \end{aligned}}$$

E. Iancu, et al hep-th/0202270

of the *colourless* dipole. The remaining, logarithmic, divergence can be cut off by hand, by introducing an infrared cutoff Λ_{QCD}. Then one can expand:

$$\int\frac{d^2k_\perp}{(2\pi)^2}\frac{1-e^{ik_\perp\cdot r_\perp}}{k_\perp^4} \simeq \int^{1/r_\perp^2}\frac{d^2k_\perp}{(2\pi)^2}\frac{1}{k_\perp^4}\frac{(k_\perp\cdot r_\perp)^2}{2} \simeq \frac{r_\perp^2}{16\pi}\ln\frac{1}{r_\perp^2\Lambda_{QCD}^2}. \qquad (2.64)$$

$$\boxed{\mathcal{N}_A(k_\perp) = \frac{N_c^2-1}{4\pi^4}\int d^2r_\perp e^{-ik_\perp\cdot r_\perp}\frac{1-\exp\left\{-\frac{1}{4}r_\perp^2Q_A^2\ln\frac{1}{r_\perp^2\Lambda_{QCD}^2}\right\}}{\alpha_s N_c r_\perp^2}, \qquad (2.68)}$$

where

$$Q_A^2 \equiv \alpha_s N_c\mu_A = \alpha_s N_c\int dx^-\lambda_A(x^-) \sim A^{1/3}. \qquad (2.69)$$

Eq. (2.68) is the complet result for the gluon density of a large nucleus in the MV model [33, 34]. To study its dependence upon $k_\perp$, one must still perform the Fourier transform, but the result can be easily anticipated:

To be more precise, the true scale which separates between the two regimes (2.70) and (2.71) is not Q_A, but rather the *saturation momentum* $Q_s(A)$ which is the reciprocal of the distance $1/r_\perp$ where the exponent in eq. (2.68) becomes of order one. Thus, this is defined as the solution to the following equation:

$$Q_s^2(A) = \frac{1}{4}\alpha_s N_c\mu_A\ln\frac{Q_s^2(A)}{\Lambda_{QCD}^2}. \qquad (2.72)$$

E. Iancu, et al hep-th/0202270

i) At high momenta $k_\perp \gg Q_A$, the integral is dominated by small distances $r_\perp \ll 1/Q_A$, and can be evaluated by expanding out the exponential. To lowest non-trivial order (which corresponds to the linear approximation), one obtains the bremsstrahlung spectrum of eq. (2.55):

$$\mathcal{N}_A(k_\perp) \propto \frac{1}{\alpha_s N_c}\frac{Q_A^2}{k_\perp^2} = \frac{\mu_A}{k_\perp^2} \quad \text{for} \quad k_\perp \gg Q_A. \tag{2.70}$$

ii) At small momenta, $k_\perp \ll Q_A$, the dominant contribution comes from large distances $r_\perp \gg 1/Q_A$, where one can simply neglect the exponential in the numerator and recognize $1/r_\perp^2$ as the Fourier transform of $\ln k_\perp^2$:

$$\mathcal{N}_A(k_\perp) \approx \frac{N_c^2-1}{4\pi^3}\frac{1}{\alpha_s N_c}\ln\frac{Q_A^2}{k_\perp^2} \quad \text{for} \quad k_\perp \ll Q_A. \tag{2.71}$$

$$\mathcal{N}_A(k_\perp) = \frac{N_c^2-1}{4\pi^4}\int d^2r_\perp e^{-ik_\perp\cdot r_\perp}\frac{1-\exp\left\{-\frac{1}{4}r_\perp^2 Q_A^2 \ln\frac{1}{r_\perp^2\Lambda_{QCD}^2}\right\}}{\alpha_s N_c r_\perp^2}$$

This is illustrated in Fig. 13.

Beware: the (cartoon) figure 13 is completely misleading!

Larry's cartoon

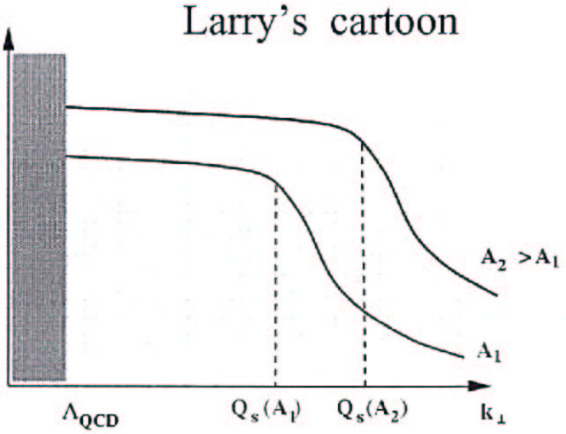

E. Iancu, et al hep-th/0202270

Figure 13: The gluon phase-space density $\mathcal{N}_A(k_\perp)$ of a large nucleus (as described by the MV model) plotted as a function of $k_\perp$.

Yuri Kovchegov and Kirill Tuchin
hep-ph/0203213 v3
Elliptic Flow paper

Bare dipole approximation fails for k>Q:

Unintegrate glue (here $Q = Q_{sat}(x, A)$ from eq 24) We show that this fails. Later section this is fixed with log 1/r modified form

$$\Phi(k, x) = \frac{KR^2}{\alpha}\int d^2 z\, e^{-ik.z}\frac{1-e^{-z^2Q^2/4}}{z^2} \qquad \text{eq. 24}$$

$$\Phi\left[\frac{k^2}{Q^2}\right]$$

Kajantie's trick $1/z^2 = \int_0^\infty e^{-sz^2} ds$

$$\Phi \propto \int_0^\infty \left(\frac{e^{-\frac{k^2}{s}}}{s} - \frac{e^{-\frac{k^2}{Q^2+s}}}{Q^2+s} \right) ds = \int_{Q^2}^\infty \frac{e^{-k^2 s}}{s} ds = E_1\left(\frac{k^2}{Q^2}\right)$$

$$\Phi(k^2 << Q^2) \sim \text{Log}\left(\frac{Q^2}{k^2}\right) \quad , \quad \Phi(k^2 >> Q^2) \sim \frac{Q^2}{k^2}\,\text{Exp}\left[-\frac{k^2}{Q^2}\right]$$

Fails DGLAP for k>Q !

Lin scale

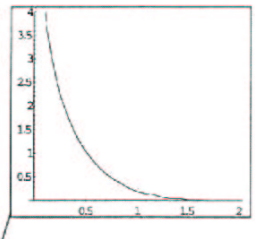

$E_1(k^2 / Q_s^2)$

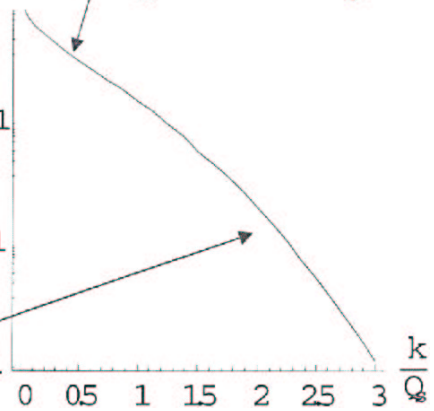

From eq 59 a log factor is introduced
Unintegrate glue here $Q = Q_{sat}(x, A)$

Log[1/z] enhanced
Dipole cross section

$$\Phi(k, x) = \frac{K R^2}{\alpha} \int^{1/\Lambda} \frac{d^2 z}{z^2} e^{-ik.z} \left(1 - e^{-\{z^2 Q^2 \mathrm{Log}(Q/z\Lambda)/\mathrm{Log}(Q/\Lambda)\}}\right)$$

Note that $z<1/\Lambda$ has now an infrared cutoff scale

Causes wiggles at RHIC

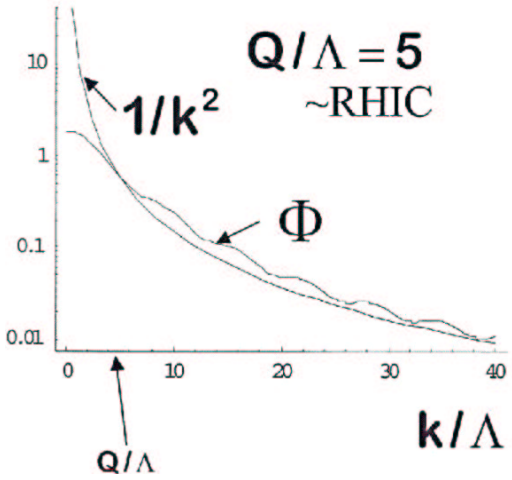

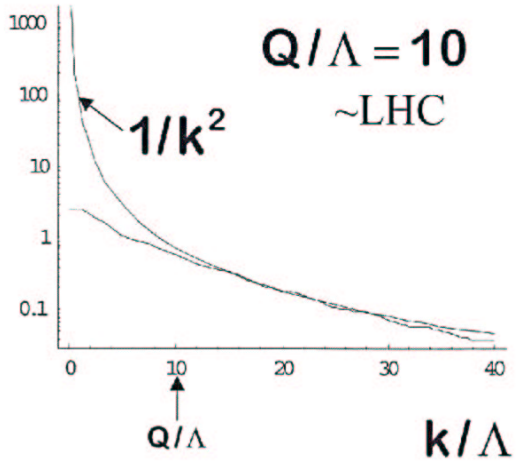

Effect of log enhanced dipole cross section

$$\Phi(k, x) = \frac{K R^2}{\alpha} \int^{1/\Lambda} \frac{d^2 z}{z^2} e^{-ik.z} \left(1 - e^{-\{z^2 Q^2 \mathrm{Log}(1/(z\Lambda)^2)\}}\right)$$

where $z>1/\Lambda$ is cutoff (dipole cross sec $\sigma(z>1/\Lambda)=0$)

```
Plot[{phed2[y, 1, .02] }, {y, .02, 4}]
```

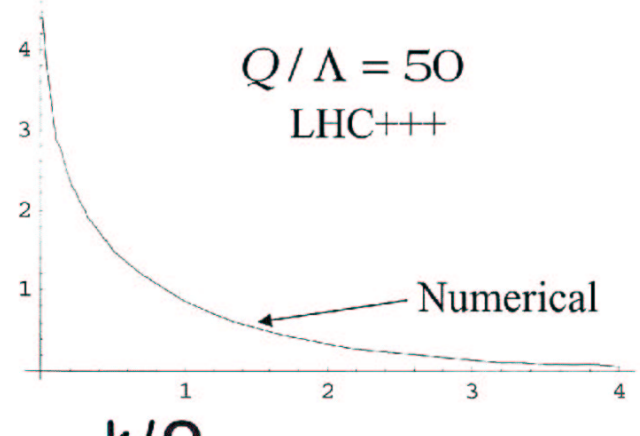

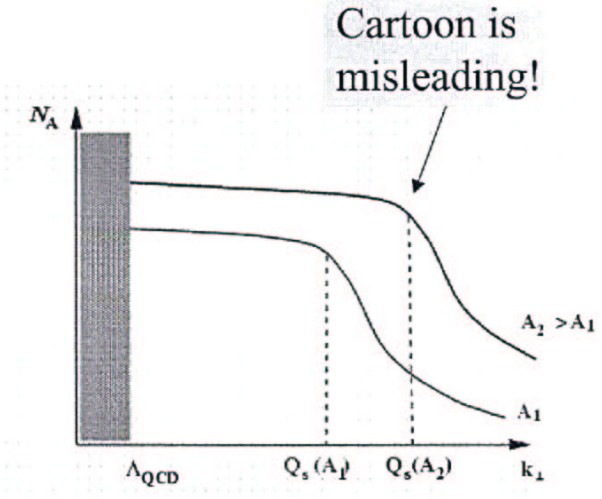

Numerical Integral is simply monotonic, no knee.

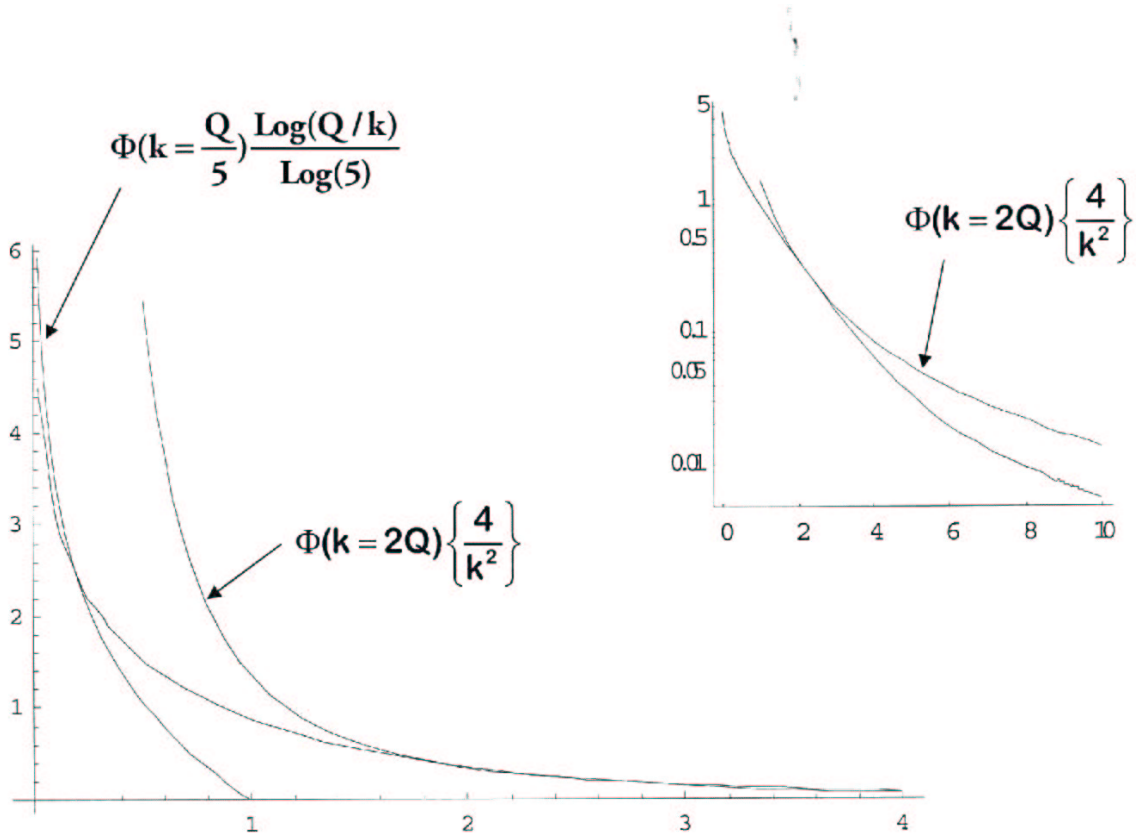

Numerical Φ is simply monotonic, no knee in either log or lin

GLR with Classical Yang Mills

$$\frac{dN}{dy d^2k} \propto \int_0^{1/\Lambda} \frac{dz}{z^3} J_0[kz] \left(1 - e^{\frac{1}{4}(-z^2) Q^2 \mathrm{Log}\left[\frac{1}{(z\Lambda)^2}\right]}\right)^2$$

Teaser

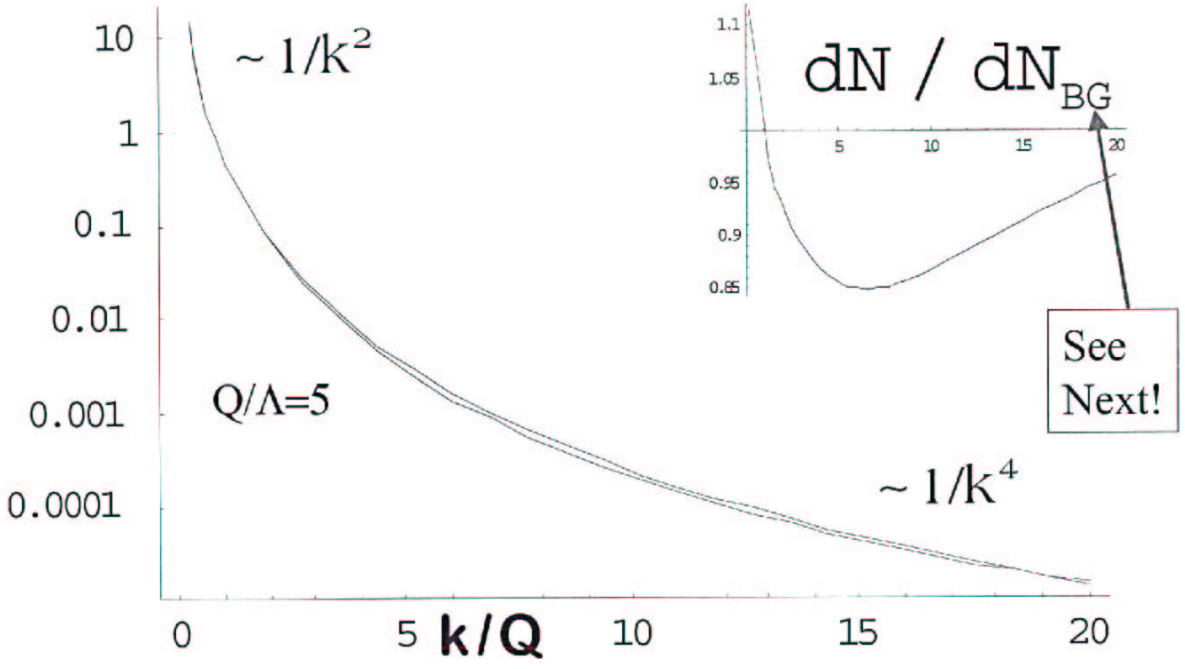

PHYSICAL REVIEW D VOLUME 25, NUMBER 3 1 FEBRUARY 1982

Hadronization by color bremsstrahlung

J. F. Gunion* and G. Bertsch†
Institute for Theoretical Physics, University of California, Santa Barbara, California 93106

$$\frac{d\sigma}{dx\,d^2q_\perp} \cong \frac{C_A\alpha_s^3}{\pi^2 x q_\perp^2}\int \frac{d^2l_\perp}{l_\perp^4}\frac{l_\perp^2}{(l_\perp-q_\perp)^2}(2)[1-f^{\rm I}_{q\bar q}((q_\perp-l_\perp)^2)](2)[1-f^{\rm II}_{q\bar q}(l_\perp^2)]$$

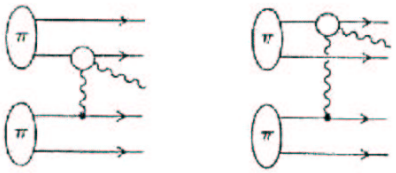

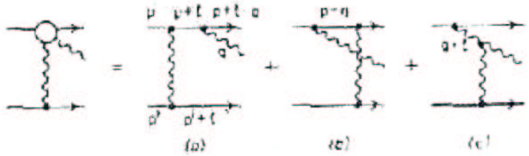

FIG. 4. Feynman diagrams for the lowest-order contributions to gluon radiation in quark scattering. Di-

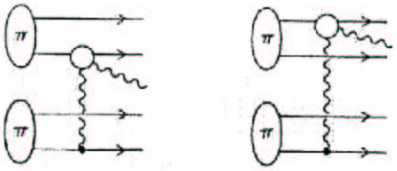

FIG. 5. Feynman diagrams for $x\to 0$ radiation in the Low-Nussinov model of hadron-hadron scattering. The circle vertex includes the three diagrams appearing in Fig. 4.

$$f_{q\bar q}(l_\perp^2)\sim(1+4l_\perp^2/m_\rho^2)^{-1}$$

$$\frac{dn}{dx\,d^2q_\perp} = \frac{C_A\alpha_s}{\pi^2 x q_\perp^2}\int \frac{d^2l_\perp[(m_\rho^2+4l_\perp^2)(m_\rho^2+4(l_\perp-q_\perp)^2)]^{-1}}{\int d^2l_\perp(m_\rho^2+4l_\perp^2)^{-2}}$$

This behaves asymptotically at large $q_\perp^2$ as

$$\frac{dn}{dx\,d^2q_\perp} \sim \frac{C_A\alpha_s}{\pi^2 x(q_\perp^2)^2} m_\rho^2 \ln q_\perp^2/m_\rho^2 .$$

Is CGC = Bertsch-Gunion Bremsstrahlung?

$$dN_{BG} \propto N_{hard}\left\langle \frac{q^2}{k^2(k-q)^2}\right\rangle \sim \left(Q_s^2R^2\right)\frac{cQ_s^2}{k^2(k^2+cQ_s^2)}$$

$dN_{CYM} = dN_{BG}(1 +- O(20\%))$ over 5 orders of magnitude!

(See plot slide 12)

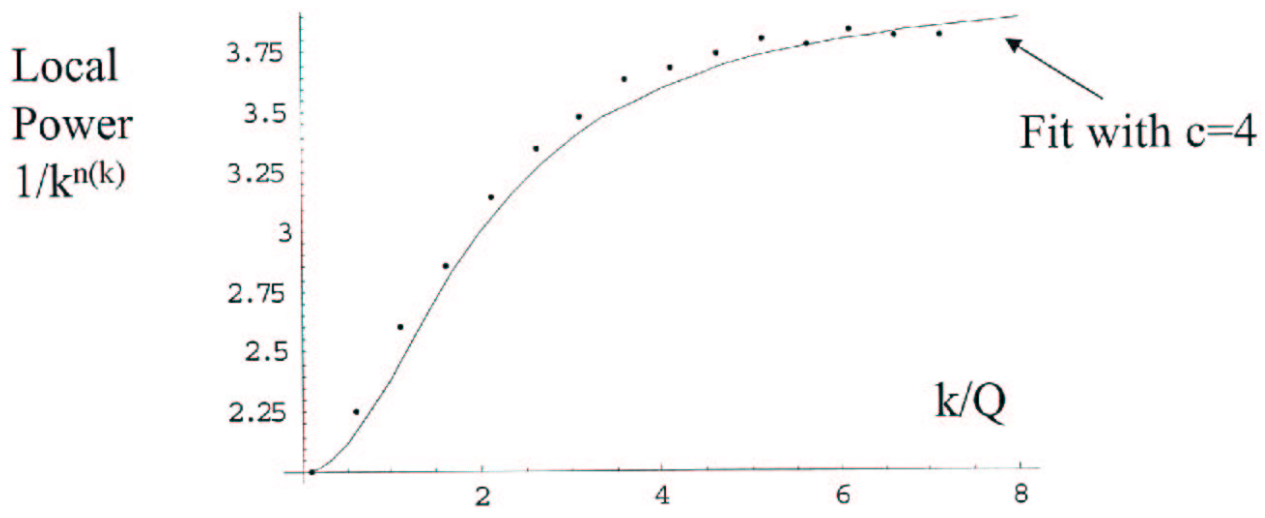

COHERENT GLUON PRODUCTION IN VERY HIGH-ENERGY HEAVY ION COLLISIONS.
Alex Krasnitz (Algarve U.), Yasushi Nara (RIKEN BNL), Raju Venugopalan (Brookhaven). Aug 2001. 4pp.
blished in **Phys.Rev.Lett.87:192302,2001**

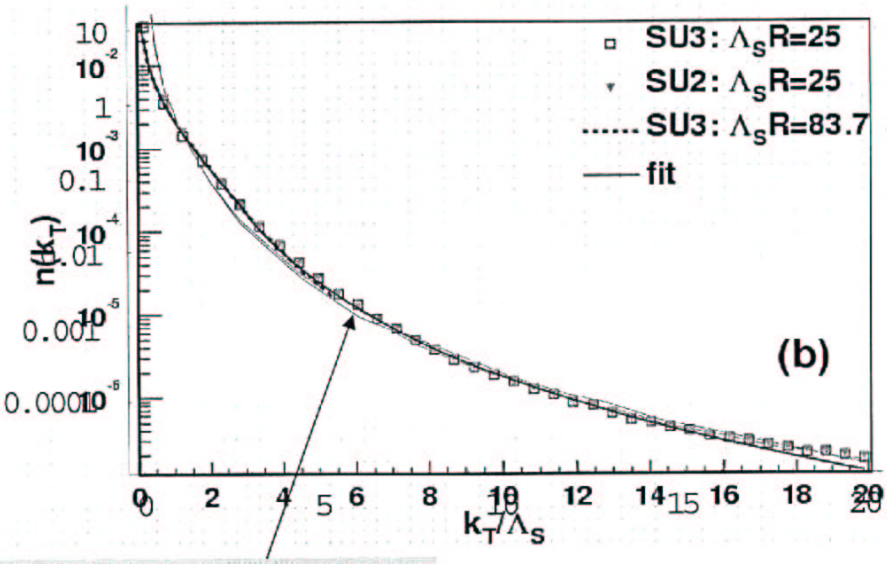

$$dN_{YM} \approx dN_{BG} \propto \frac{4Q_s^2}{k^2(k^2+4Q_s^2)}$$

BG fits lattice YM incredibly well

COHERENT GLUON PRODUCTION IN VERY HIGH-ENERGY HEAVY ION COLLISIONS.
Alex Krasnitz (Algarve U.), Yasushi Nara (RIKEN BNL), Raju Venugopalan (Brookhaven). Aug 2001. 4pp.
blished in **Phys.Rev.Lett.87:192302,2001**

$$\frac{1}{\pi R^2}\frac{dN}{d\eta d^2k_T} = \frac{1}{g^2}\tilde{f}_n(k_T/\Lambda_s)\,, \qquad (6)$$

where $\tilde{f}_n(k_T/\Lambda_s)$ is

$$\tilde{f}_n = \begin{cases} a_1\left[\exp\left(\sqrt{k_T^2+m^2}/T_{\rm eff}\right)-1\right]^{-1} & (k_T/\Lambda_s \le 3) \\ a_2\,\Lambda_s{}^4\log(4\pi k_T/\Lambda_s)k_T^{-4} & (k_T/\Lambda_s > 3) \end{cases} \qquad (7)$$

with $a_1 = 0.0295$, $m = 0.067\Lambda_s$, $T_{\rm eff} = 0.93\Lambda_s$, and $a_2 = 0.0343$. At low momenta, the functional form is approximately that of a Bose-Einstein distribution in two dimensions even though the underlying dynamics is that of classical fields. The functional form at high momen-

$$\frac{dE_T^h}{d\eta}|_{\eta=0} = \frac{\pi}{g^2}\frac{1}{\kappa_{work}} f_E(\Lambda_s R)\,\Lambda_s\,(\Lambda_s R)^2\,,$$
$$\frac{dN^h}{d\eta}|_{\eta=0} = \frac{\pi\kappa_{inel}}{g^2} f_N(\Lambda_s R)\,(\Lambda_s R)^2\,. \qquad (9)$$

From the RHIC data at $\sqrt{s_{NN}} = 130$ GeV, we have $dN^h/d\eta|_{\eta=0} \sim 1000$ for central collisions [25–28]. For $g = 2$ ($\alpha_s = 0.33$), $\pi R^2 = 148$ fm^2, and $f_N = 0.3$, we have $\kappa_{inel}\Lambda_s^2 = 3.5$ GeV^2. Now, from Eq. (8), the ratio $R^h = dE_T^h/d\eta/dN^h/d\eta$ is, since $f_E/f_N = 1.66$, $R^h = 1.66\Lambda_s/\kappa_{work}/\kappa_{inel}$. The experimental value [26] for $\sqrt{s_{NN}} = 130$ GeV is $R^h = 0.5$ GeV. Now, if we assume that there is no work done due to thermalization, $\kappa_{work} = 1$, we obtain from the two conditions $\Lambda_s = 1.02$ GeV and $\kappa_{inel} = 3.4$ as the values that give agreement with the data. The latter value is the maximal amount of inelastic gluon production possible. Alternatively, if we assume hydrodynamic work is done, one obtains $\kappa_{work} = (\tau_f/\tau_i)^{1/3}$, where τ_f and τ_i are the final and initial times of hydrodynamic expansion respectively. This gives us $\kappa_{work} \approx 2$. Following the same analysis as previously, we obtain $\Lambda_s = 1.28$ GeV and $\kappa_{inel} = 2.13$. Thus, within the CGC approach, we are able to place bounds on both the saturation scale and on the amount of inelastic gluon production at RHIC energies. An independent method

Summary:

1) CYM (with log enhanced dipole cross sec) predicts a monotonically decreasing gluon pt distribution with very smooth cross over from 1/k^2 to 1/k^4

2) CYM is weak kneed. There is NO knee at pt ~ Qsat! Cartoon dxG(x,Q^2)/dQ^2 theta functions are not predicted by CYM. Hence RHIC predictions with cartoons must be revisited.

3) Analytic CYM ~ lattice YM can be surprisingly well fit with simple Bertsch-Gunion form

$$dN_{BG} \sim \frac{c Q_s^4}{k^2(k^2 + c Q_s^2)}$$

Summary 2:

4) Latest lattice YM results require final state gluon multiplication $\kappa_{inel} \sim$ 2-3 as well hydrodynamic work $\kappa_{work} \sim$2-3 to reduce ET

This means that CYM initial conditions are not ***observed experimentally*** at RHIC

5) Other brand X (***Poly-Unsaturated***) Models: HIJING, AMPT …
also predict similar initial gluon multiplicities as well as final hadron spectra

6) Problem is that Q~ 1 GeV at RHIC.